JOURNAL OF AGRICULTURAL AND FOOD CHEMISTRY

Article

pubs.acs.org/JAFC

Graphene Enhances Cellular Proliferation through Activating the Epidermal Growth Factor Receptor

Wei Liu,[†] Cheng Sun,[‡] Chunyang Liao,[‡] Lin Cui,[‡] Haishan Li,[†] Guangbo Qu,[‡] Wenlian Yu,[†] Naining Song,[†] Yuan Cui,[†] Zheng Wang,[†] Wenping Xie,[†] Huiming Chen,*[,†] and Qunfang Zhou*[,‡]

[†]Institute of Chemical Safety, Chinese Academy of Inspection and Quarantine, Beijing 100124, People's Republic of China

[‡]Research Center for Eco-Environmental Sciences, Chinese Academy of Sciences, Beijing 100085, People's Republic of China

Supporting Information

ABSTRACT: Graphene has promising applications in food packaging, water purification, and detective sensors for contamination monitoring. However, the biological effects of graphene are not fully understood. It is necessary to clarify the potential risks of graphene exposure to humans through diverse routes, such as foods. In the present study, graphene, as the model nanomaterial, was used to test its potential effects on the cell proliferation based on multiple representative cell lines, including HepG2, A549, MCF-7, and HeLa cells. Graphene was characterized by Raman spectroscopy, particle size analysis, atomic force microscopy, and transmission electron microscopy. The cellular responses to graphene exposure were evaluated using flow cytometry, 3-(4,5-dimethylthiazol-2-yl)-2,5-diphenyltetrazolium bromide, and alamarBlue assays. Rat cerebral astrocyte cultures, as the non-cancer cells, were used to assess the potential cytotoxicity of graphene as well. The results showed that graphene stimulation enhanced cell proliferation in all tested cell cultures and the highest elevation in cell growth was up to 60%. A western blot assay showed that the expression of epidermal growth factor (EGF) was upregulated upon graphene treatment. The phosphorylation of EGF receptor (EGFR) and the downstream proteins, ShC and extracellular regulating kinase (ERK), were remarkably induced, indicating that the activation of the mitogen-activated protein kinase (MAPK)/ERK signaling pathway was triggered. The activation of PI3 kinase p85 and AKT showed that the PI3K/AKT signaling pathway was also involved in graphene-induced cell proliferation, causing the increase of cell ratios in the G2/M phase. No influences on cell apoptosis were observed in graphene-treated cells when compared to the negative controls, proving the low cytotoxicity of this emerging nanomaterial. The findings in this study revealed the potential cellular biological effect of graphene, which may give useful hints on its biosafety evaluation and the further exploration of the bioapplication.

KEYWORDS: *graphene, cell proliferation, EGFR, cytotoxicity, biosafety*

INTRODUCTION

Graphene is a kind of two-dimensional nanomaterial, and it is composed of sp^2-hybridized carbon atoms hexagonally arranged in single-atom thickness. It has a large surface area on both sides of the planar axis and possesses unique electrical, thermal, and mechanical characters.[1] Since the production of graphene layers was proposed by mechanically peeling sheets off graphite crystals in 2004, the application of this emerging nanomaterial has been widely explored in several fields, such as electronics and biomedicine.[2,3] The usage of graphene in food packaging is becoming more and more popular because graphene nanoplates are heat-resistant and can efficiently prevent the migration of oxygen, CO_2, and water vapor.[4] Graphene-based material was also reported to kill pathogenic microbes in food and drinking water.[5−8] Graphene-based sensors are effective for the contamination monitoring in food and water.[9,10] All of these usages evidently cause the exposure of graphene to humans. It is thus necessary to understand the potential biological effects of this emerging nanomaterial.

In view of the cytotoxicity of graphene-based materials, there is no consensus in recent studies. Some people believe that the derivatives of graphene are highly biocompatible without any significant toxicity, while others pointed out that obvious cytotoxicity was induced by this kind of nanomaterial in several cell lines.[11−14] For instance, Ryoo et al. showed that graphene substrates improved gene transfection efficacy in NIH-3T3 fibroblasts without inducing notable deleterious effects.[14] Chang et al. found that graphene oxide (GO) did not enter A549 cells and showed no obvious toxicity to A549 cells.[15] On the contrary, Wang et al. demonstrated that water-soluble GO had obvious toxicity to human fibroblast cells, such as decreasing cell adhesion, inducing cell apoptosis, and entering into lysosomes, mitochondria, endoplasm, and cell nucleus when the dose was higher than 50 μg/mL.[16] Biris et al. demonstrated that graphene sheets (GS) induced cytotoxic effects on phaeochromocytoma (PC-12) cells, while its toxicity was much lower than carbon nanotubes.[17] Different cytotoxicities were observed for graphene in diverse cell types. Qu et al. demonstrated that GO inhibited the proliferations of J774A.1 and RAW 264.7 cells at the doses ranging from 2.5 to 80 μg/mL, but they did not observe any impairments induced by GO at similar doses on the cell growth or survival of the other tested cell lines, including mouse Hepa 1−6 hepatocytes, human Hepa

Received: December 18, 2015
Revised: June 20, 2016
Accepted: June 20, 2016
Published: June 20, 2016

ACS Publications © 2016 American Chemical Society

DOI: 10.1021/acs.jafc.5b05923
J. Agric. Food Chem. 2016, 64, 5909−5918

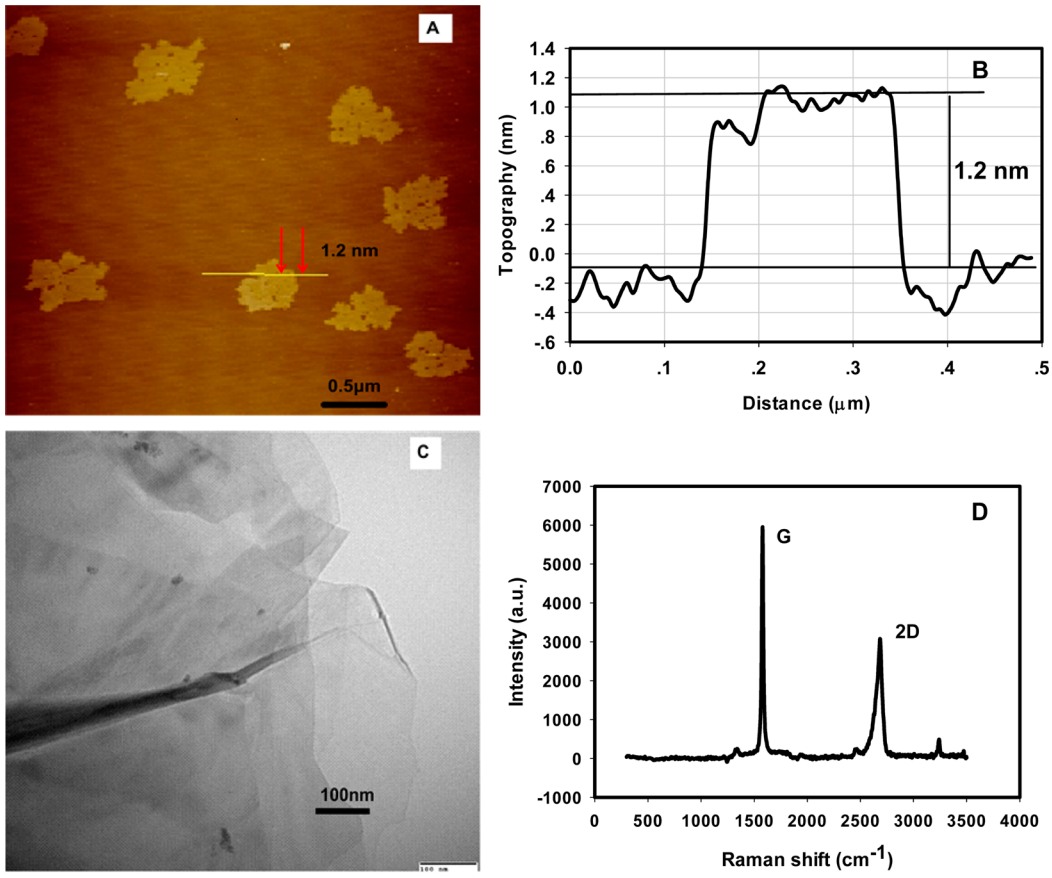

Figure 1. Characterization of the graphene: (A) AFM image, (B) AFM topography, (C) TEM image, and (D) Raman spectrum.

G2 hepatocytes, or human MB-MDA-231 breast cancer cells.[18] Altogether, most of the toxicological studies focused on the exploration of the potential biological effects of GO materials, and people believed that GO materials were more toxic than graphene because they could form stable colloidal suspensions in cell culture systems.[19] However, it was pitifully inadequate to make the arbitrary conclusion about the exposure risks of graphene based on the data from GO materials regarding its current wide applications and the distinct characters of these two kinds of nanomaterials.

The aim of this study was to investigate the cellular biological effects of a well-prepared graphene. The cell proliferations of multiple cell cultures were first screened by graphene stimulations. The most interesting finding was that the graphene treatment caused significant elevation in cell proliferation in all tested cell cultures. The investigation on the underlying molecular mechanisms showed that both mitogen-activated protein kinase (MAPK)/extracellular regulating kinase (ERK) and PI3K/AKT signaling pathways were involved in graphene-induced cell growth. To our knowledge, this was the first report that fully elucidated graphene-enhanced cellular proliferation on the molecular mechanisms.

MATERIALS AND METHODS

Graphene Preparation and Characterization. Graphene is purchased from XFNANO Materials Tech Co., Ltd. (Nanjing, China). Stocking graphene suspension is prepared in dimethyl sulfoxide (DMSO) or cell culture medium with 0.5% fetal bovine serum (FBS) (for cell apoptosis and cell cycle assays) at a concentration of 1×10^3 μg/mL. The suspension is dispersed by ultrasonic for 5 min to obtain homogeneous concentration before treatment.

Table 1. ζ Potentials of the Graphene in Different Suspensions

medium	ζ potential (mV)
water	−12.58 ± 3.30
DMSO	−9.33 ± 1.84
RPMI1640 cell culture medium with 10% FBS	−0.656 ± 1.49

The graphene was characterized by Raman spectrum (Horiba Jobin Yvon LabRAM HR800, Japan). ζ potential was measured at 10 μg/mL in water, DMSO, and RPMI1640 medium with 10% FBS by a laser particle size analyzer (Malvern Nano ZS, Nalvern, U.K.). The morphologies of graphene were observed by transmission electron microscopy (TEM, Hitachi H-7500, Japan) and atomic force microscopy (AFM, Veeco Dimension 3100, Plainview, NY).

Cell Culture. The five types of commercially available cell lines used in this study were human lung adenocarcinoma ephithelial cells (A549), human hepatocellular carcinoma cells (HepG2), human breast adenocarcinoma cells (MCF-7), human cervical carcinoma cells (HeLa), and Chinese hamster ovary cells (CHO-K1). A549, HepG2, and HeLa cells were maintained in RPMI1640 medium (Hyclone, Logan, UT). MCF-7 cells were cultured in Dulbecco's modified Eagle's medium (DMEM, Hyclone), and CHO-K1 cells were cultured in Dulbecco's modified Eagle's medium supplied with F12 (DMEM/F12, Hyclone). The primary cultured astrocyte cells were kindly provided by Dr. Qunfang Zhou from the Research Center for Eco-Environmental Sciences (RCEES), Chinese Academy of Sciences (CAS), Beijing, China, and maintained in DMEM/F12 (Hyclone).[20] All media were supplemented with 10% FBS (Gibco, Grand Island, NY) and 100 units/mL penicillin/streptomycin (Gibco). All cell lines were grown at 37 °C in a 5% CO_2 humidified environment. The cells at a logarithmic phase of growth were used for the exposure tests.

DOI: 10.1021/acs.jafc.5b05923
J. Agric. Food Chem. 2016, 64, 5909−5918

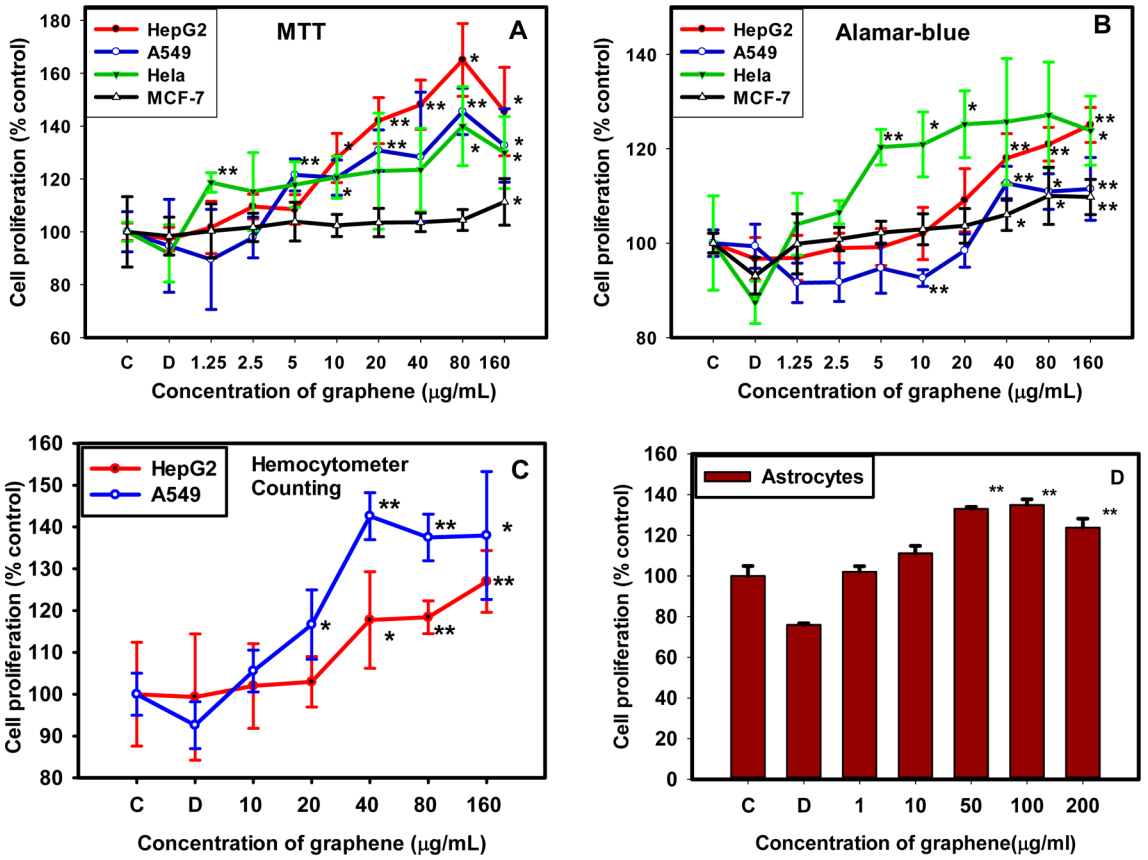

Figure 2. Cell proliferation in different cell lines exposed to the graphene: (A) MTT assay, (B) alamarBlue assay, (C) hemocytometer counting, and (D) cell proliferation of rat cerebral astrocytes exposed to the graphene. The groups of panels C and D marked in abscissa stand for the negative control and 1% DMSO solvent group, respectively.

Cell Viability. The cell viability was examined by three different methods. For the 3-(4,5-dimethylthiazol-2-yl)-2,5-diphenyltetrazolium bromide (MTT) assay, the protocol was adapted from Mosmann et al.[21] Cells were exposed to graphene of 1.25, 2.5, 5, 10, 20, 40, 80, and 160 μg/mL for 24 h. At the end of exposure, 150 μL MTT (Amresco, Solon, OH) solutions (0.5 mg/mL in cell culture medium) were added to each well and the cells were incubated at 37 °C for 4 h. After incubation, MTT solution was aspirated and the cells were treated with 150 μL of DMSO (Amresco). The plates were slightly shaken at room temperature until the crystals were dissolved. Absorbance was measured at 490 nm using a multimode microplate spectrophotometer (Varioskan Flash, Thermo Scientific, Waltham, MA).

For the alamarBlue assay, cells were exposed to graphene of 1.25, 2.5, 5, 10, 20, 40, 80, and 160 μg/mL for 24 h. At the end of exposure, $^{1}/_{10}$ volume of alamarBlue reagent (Life Technologies) was added directly to cells in culture medium. Then, cells were incubated for 2 h at 37 °C in the dark. Fluorescence emission at 590 nm (excited at 540 nm) was measured by a multimode microplate spectrophotometer (Varioskan Flash, Thermo Scientific, Waltham, MA).

For cell counting, cells were seeded in 6-well plates with 10^5 cells/well. After culturing for 12 h, cells were treated with graphene at doses of 10, 20, 40, and 80 μg/mL. After 24 h, live cell counting was performed with a hemocytometer after trypan blue staining.

Cell Apoptosis and Cell Cycle. Cell apoptosis and necrosis were analyzed by double staining with Annexin V-FITC and propidium iodide (PI), and 100 units/mL TNF-a (Calbiochem, San Diego, CA) was used as the positive control. After 24 h of exposure, the cells were collected and stained using the Annexin V-FITC Apoptosis Detection Kit (Bender, Austria). Then, the samples were detected by the flow cytometer (FACSCalibur, Becton Dickenson, San Jose, CA).

Cell cycle progression was also analyzed using the flow cytometer. Cells were seeded in 6-well plates with 10^5 cells/well, starved for 48 h in medium with 0.5% FBS for synchronization, then changed to normal medium, and treated with graphene. After 24 h of exposure, the collected cells were washed by PBS and fixed using 70% ethanol overnight. Ethanol was removed by centrifugation (1500 rpm for 5 min), and the cells were washed twice with PBS. Cells were then resuspended in PBS containing RNase (1 mg/mL, Sigma, St. Louis, MO) and PI (50 mg/mL, Sigma), kept at 37 °C in the dark for 30 min, and then analyzed by measuring the amount of PI-labeled DNA on the flow cytometer.

Western Bloting. Cells were seeded in 6-well plates with 10^5 cells/well and treated with 0, 10, 20, 40 μg/mL graphene, and DMSO was used as the solvent control with the same dose as in 40 μg/mL graphene (0.25%). After treatment for 24 h, cells was washed with PBS 3 times and lysed with radioimmunoprecipitation assay (RIPA) lysis buffer. The same amount of protein extracts was loaded for the separation on 10% sodium dodecyl sulfate−polyacrylamide gel electrophoresis (SDS−PAGE) and then transferred to nitrocellulose membranes. The membranes were blocked with 5% non-fat milk in Tris-buffered saline with Tween 20 (TBST) at room temperature for 1 h. The primary antibody was used at 1:1000 dilution and incubated overnight at 4 °C with gentle shake. The secondary antibody was used at 1:1000 dilution and incubated for 2 h at room temperature. Blots were developed using enhanced chemiluminescence. The tested proteins were phospho-epidermal growth factor receptor (EGFR), phospho-ERK (P-ERK), ERK, phospho-PI3 kinases p85, phospho-AKT, AKT, phospho-ShC, and β-actin. All of the antibodies were purchased from Cell Signaling Technology.

miRNA Silencing and Reverse Transcription Polymerase Chain Reaction (RT-PCR) Analysis. HepG2 cells were seeded in 6-well plates with 10^5 cells/well and transfected with (1) miRNA-7 (synthesized by Sangon Biotech, Shanghai, China) in Lipofectamine2000 (Lipo2000, Invitrogen) and (2) negative control with Cy3 tag (Cy3-NC, synthesized by Sangon Biotech, Shanghai, China) in Lipo2000. Cells were continuously incubated for 24 h after transfection.

DOI: 10.1021/acs.jafc.5b05923
J. Agric. Food Chem. 2016, 64, 5909−5918

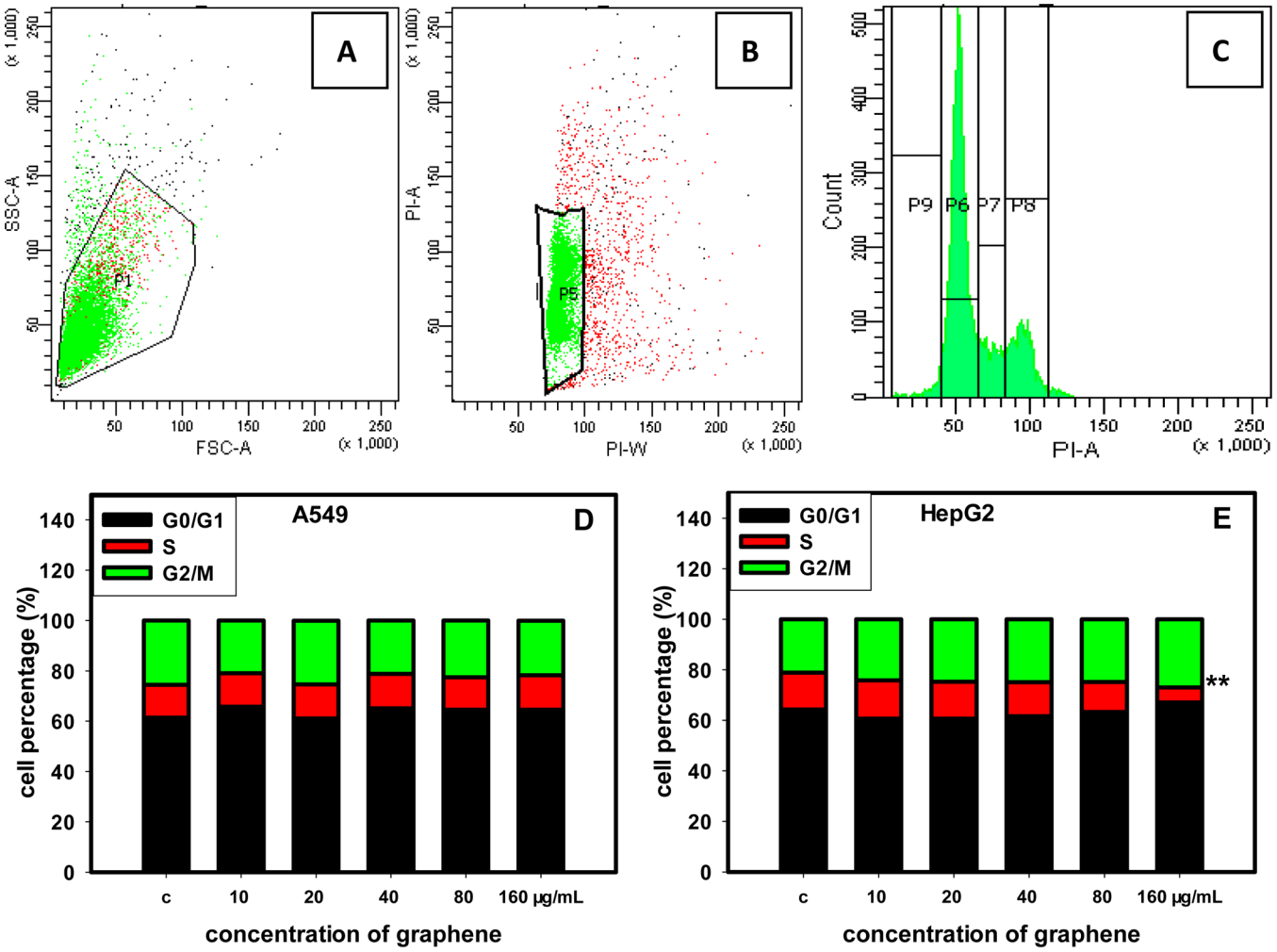

Figure 3. Cell cycle changes after graphene treatment. (A–C) Gates in which cells were analyzed. The data were from the samples in the group of A549 treated with 80 μg/mL graphene. (D) Cell cycle changes in A549 cells treated by different doses of graphene. (E) Cell cycle changes in HepG2 cells treated by different doses of graphene. (**) $p < 0.01$.

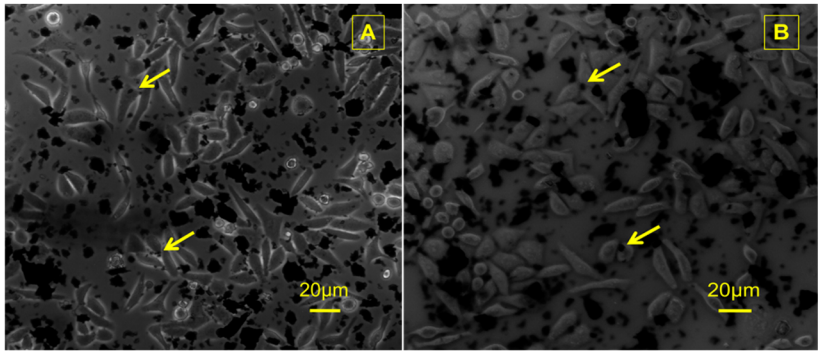

Figure 4. Microscopic images of HepG2 cells treated with 40 μg/mL graphene for 24 h: (A) light field and (B) differential interference contrast (DIC) image.

The transfection efficiency was investigated by confocal laser scanning microscopy (CLSM, Zeiss 510, Germany).

Transfected cells were treated with 40 μg/mL graphene. Relative quantifications of mRNA expression in the genes EGFR, PI3K, and Akt were calculated using the RT-PCR assay.

Total RNAs were extracted from cells using Trizol (Invitrogen). RT-PCR analysis was performed as described in ref 22. Glyceraldehyde 3-phosphate dehydrogenase (GAPDH) was used as an internal control. Primers are as follows: GAPDH forward, 5′-CAT CAG CAA TGC CTC CTG CAC-3′ and reverse, 5′-TGA GTC CTT CCA CGA TAC CAA AGTT-3′; EGFR forward, 5′-CTT GAT TCC AGT GGT TCT GCT TC-3′ and reverse, 5′-CAT CCC CTC CGT TTC TTC TTT-3′; PI3K forward, 5′-CTG TGT GGG ACT TAT TGA GGT GGT-3′ and reverse, 5′-ACT GAT GTA GTG TGT GGC TGT TGA-3′; and Akt forward, 5′-TGT GAA GGA GGG TTG GCT GC-3′ and reverse, 5′-ACT GCG CCA CAG AGA AGT TGTT-3′.

Statistical Analysis. The difference of experimental data between two groups was assessed using the two-tailed Student's t test. Data

DOI: 10.1021/acs.jafc.5b05923
J. Agric. Food Chem. 2016, 64, 5909–5918

were shown as the mean ± standard deviation (SD) ($n \geq 3$). $p < 0.05$ was considered statistically significant.

RESULTS AND DISCUSSION

Characterization of Graphene. The commercially available graphene was specified with no functionalization or oxidation. Careful characterization was performed before it was submitted to the cell stimulations. The results based on AFM observation showed that the thickness of this graphene was about 1.2 nm (panels A and B of Figure 1). The morphology provided by TEM demonstrated that the graphene consisted of ultrathin layers (Figure 1C). Raman spectrum analysis showed the featured peaks of graphene at 1580 cm^{-1} (G peak) and 2680 cm^{-1} (2D peak) (Figure 1D), indicating the character of multilayers for this graphene.[23,24] This result was consistent with the thickness of an individual GS (1.2 nm) obtained by AFM measurement. The characterization of ζ potential showed that this graphene was negatively charged in water and DMSO, while it turned nearly neutral in cell culture medium (Table 1). The stability of graphene suspensions was evaluated, and the results showed that graphene was well-dispersed in DMSO and cell culture medium after ultrasonics for 5 min.

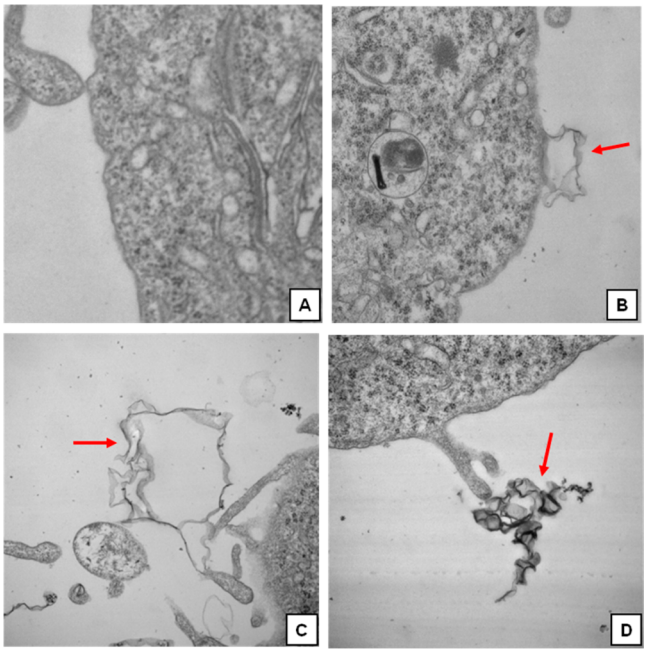

Figure 5. TEM image of (A) edge of HepG2 cellular membrane in the control group and (B–D) GS (indicated by red arrow) around HepG2 cells in groups treated with 40 μg/mL graphene for 24 h. Magnification: (A and B) 25000× and (C and D) 30000×.

Graphene-Induced Cell Proliferation in Diverse Cell Cultures. As reported, liver and lung are the important target tissues in which graphene family nanomaterials may bioaccumulate and induce damnification.[25] A long-term *in vivo* study revealed that the graphene quantum dots mainly accumulated in liver, spleen, lung, kidney, and tumor sites.[26] Graphene accumulated initially in the reticuloendothelial system (RES), liver, and spleen after intravenous injection.[27] Graphene oxides at a dose of 0.4 mg induced granulomas in the lung, liver, spleen, and kidney in mice.[16] Moreover, GOs showed good biocompatibility with red blood cells.[28] *In vivo* fluorescence imaging revealed that graphene had high uptaken in the tumor in several xenograft tumor mouse models.[29] On the basis of the liver/lung targeting and tumor uptake of graphene, we chose cell lines (HepG2 and A549) derived from liver and lung as the main models to study the *in vitro* toxicity of graphene. Several other cells were also selected to discuss the cell type selection for the graphene cytoxicity test.

To assess the potential cellular biological effects of the graphene, we performed 24 h stimulation on four cell lines, including HepG2, A549, HeLa, and MCF-7, with the graphene at a series of concentration gradients (1.25–160 μg/mL). The cell viability based on the MTT assay showed that obvious cell proliferation was induced for all four cell lines in the tested dose range (Figure 2A). Comparatively, three cell lines, including HepG2, A549 and HeLa cells, showed more sensitivity to graphene treatment when compared to MCF-7. For example, a significant increase in cell proliferation was observed in HepG2 cells exposed to 10 μg/mL graphene, while the elevation in cell growth did not become significant for MCF-7 until it was stimulated by 160 μg/mL graphene. An approximate 20–60% cell proliferation increase was observed in HepG2 in the tested range of 10–160 μg/mL graphene, and it climaxed at the stimulation of 80 μg/mL graphene with the increased ratio of 60%. The typical dose-dependent manner was clearly exhibited in this cellular response induced by graphene. Likewise, A549 and HeLa cells responded to graphene exposure in a way similar to HepG2.

Nevertheless, the argument was proposed by Liao et al. that the MTT assay would be influenced by GS/GO materials because they could reduce the $[MTT]^{+}$ cations by donating the electrons.[30] The potential disturbance of graphene on the MTT

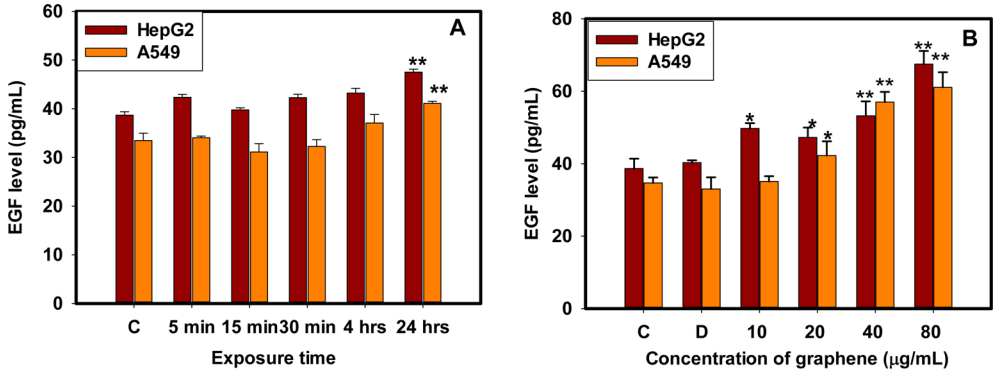

Figure 6. Graphene increased the secretion of EGF in HepG2 and A549 cell culture medium systems: (A) time course for EGF secretion upon the treatments with 20 μg/mL graphene and (B) dose–response for EGF secretion upon 24 h stimulations.

DOI: 10.1021/acs.jafc.5b05923
J. Agric. Food Chem. 2016, 64, 5909–5918

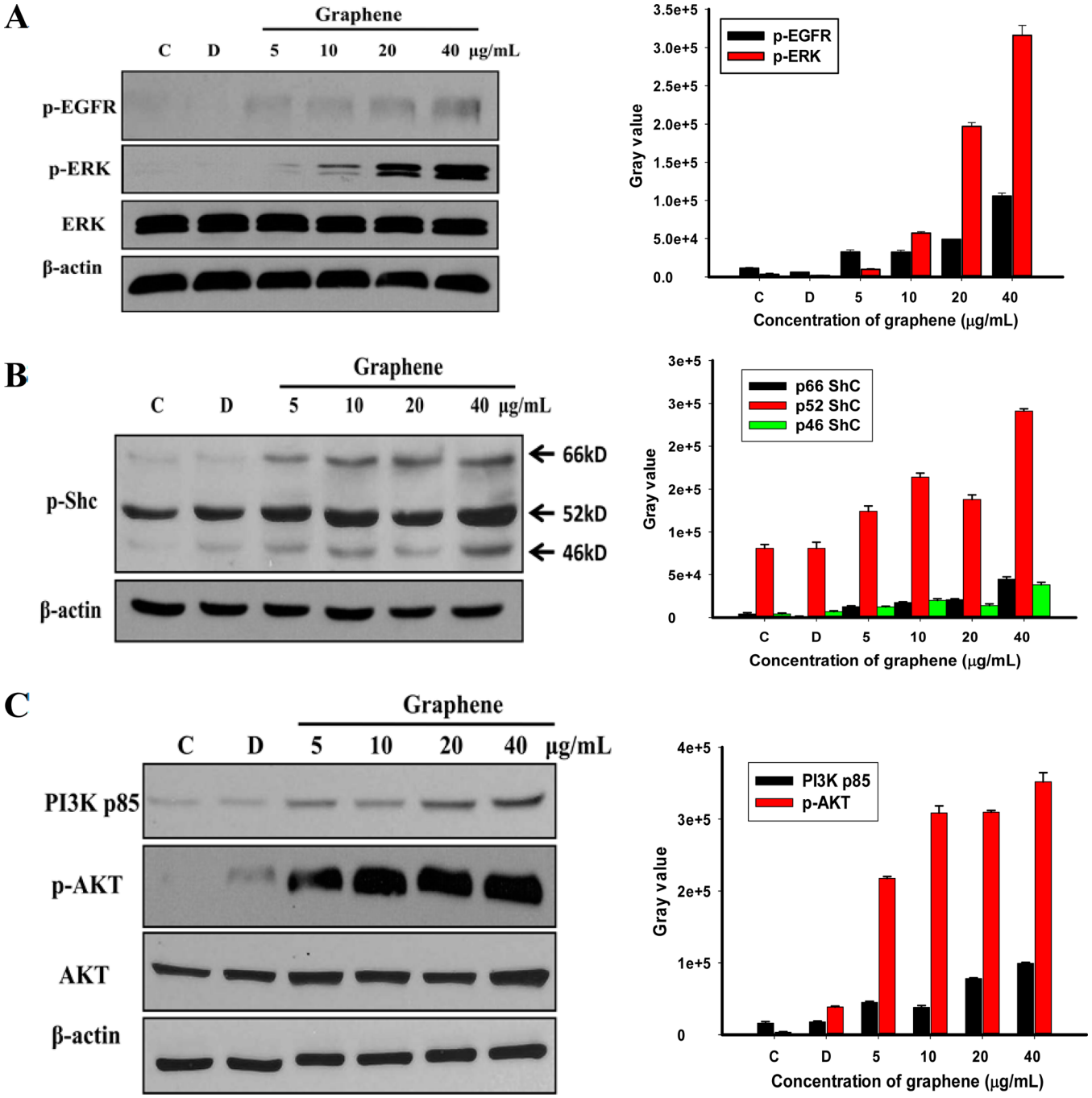

Figure 7. Activation of MAPK/ERK and PI3K/AKT pathways in HepG2 cells treated with different doses of graphene for 24 h. The histogram showed the calculated gray value of corresponding bands in the western blotting results. *β*-Actin was used as the loading control. (A) Protein levels of phosphorylated EGFR, phosphorylated ERK and total ERK. (B) Protein level of phosphorylated ShC. (C) Protein levels of PI3K p85 subunit, phosphorylated AKT, and total AKT. C and D in the concentration line stand for untreated control and 0.25% DMSO (equal to DMSO in the 40 μg/mL treated group), respectively.

assay was evaluated by the direct incubation of this nanomaterial with the MTT dye, and the result showed that no effect was observed during the tested range of 0−160 μg/mL graphene (data not shown). This confirmed that the cell proliferation induced by graphene observed above was real instead of the false-positive results from the failure of the MTT assay in evaluation of the effects of some nanomaterials.

The cellular phenotype of graphene-induced cell proliferation was further tested by some alternative methods, including the alamarBlue assay and hemocytometer counting. The results in panels B and C of Figure 2 showed that the trends similar in cell proliferation were exhibited in all tested cell cultures upon graphene treatments, although the sensitivities in cell responses were varied. These findings further confirmed the phenotype of the enhanced cellular proliferation upon graphene stimulation.

As we know, those four cell lines used above are all derived from diverse tumor tissues and may have some specific distinct characters when compared to the normal tissue cells. The subcultures from the primary rat cerebral astrocytes were used to evaluate the potential effects of graphene on normal tissue cells.

DOI: 10.1021/acs.jafc.5b05923
J. Agric. Food Chem. 2016, 64, 5909−5918

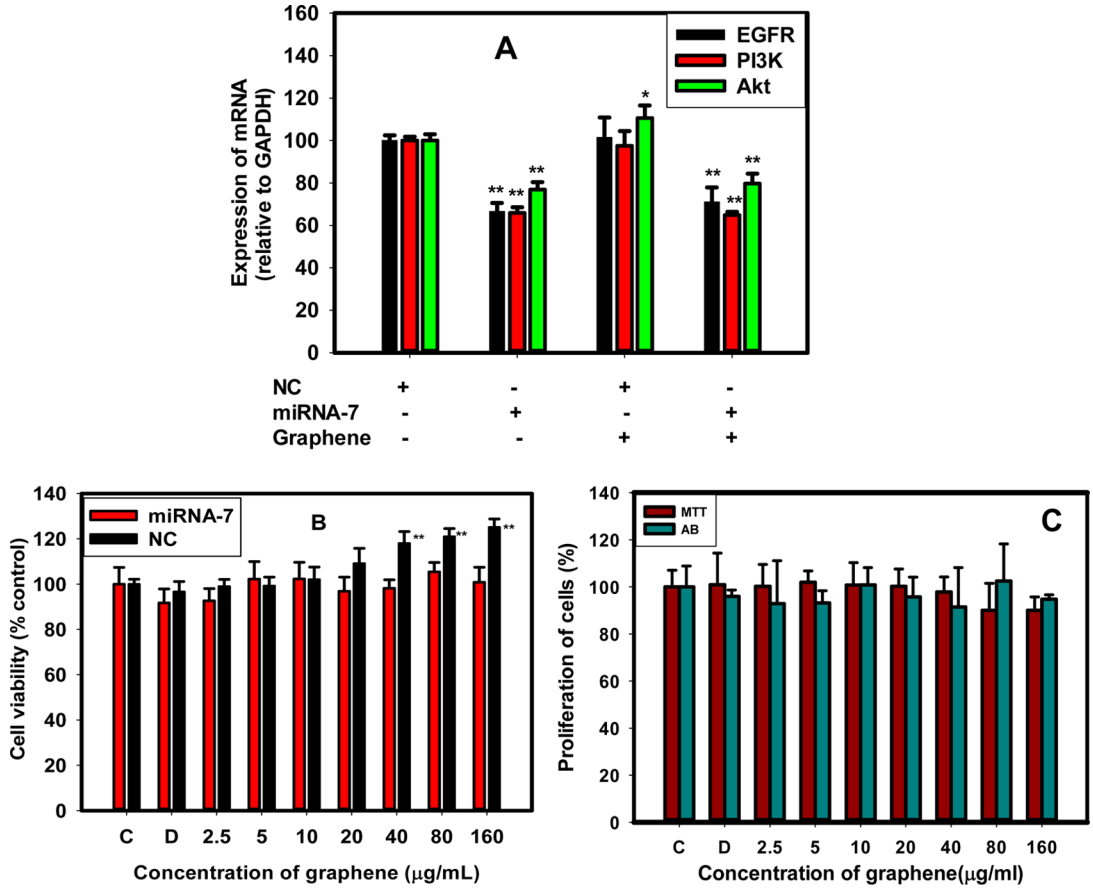

Figure 8. Validation of graphene-enhanced cellular proliferation through the EGFR pathway. (A) mRNA expressions of EGFR/PI3K/Akt in HepG2 cells with or without miRNA-7 transfection and graphene treatment. (**) $p < 0.01$ and (*) $p < 0.05$. NC = negative control. (B) Cellular proliferation of HepG2 upon graphene treatment after NC/miRNA-7 transfection. (**) $p < 0.01$. (C) Cellular proliferation of the EGFR negative cell line CHO-K1 upon 24 h of treatment by different doses of graphene. The groups of panels C and D marked in abscissa stand for the negative control and 1% DMSO solvent group, respectively.

The results from the alamarBlue assay showed that graphene stimulation caused the significant increase in the proliferation of astrocytes as well (Figure 2D), and this cellular response was also elevated in the dose-dependent manner. This was consistent with the findings from the other tested cell lines, proving that graphene-induced cell proliferation occurred in both tumor-derived cell lines and normal cells.

Effects of Graphene on Cell Cycle Progression. We investigated the apoptosis and necrosis using FITC-Annexin V and PI staining and detected it by flow cytometry. No change was observed between cells treated with and without graphene (data not shown). The cell cycle was detected by flow cytometry and PI staining. We found no obvious changes in phase percentage in graphene-treated A549 cells in comparison to the untreated cells (Figure 3D). While in HepG2 cells, there is an increase of G2/M percentages and a concomitantly decrease of S fractions (Figure 3E). This result revealed the enhancement of transition from the S phase to the G2/M phase upon graphene treatment, which would also contribute to the cellular proliferation.

Attachment of Graphene on the Cell Membrane. Previous studies[31] have indicated that graphene exhibited excellent compatibility with red blood cells and platelets. It did not disturb the plasma coagulation pathways. Minimal alterations were induced in the cytokine expression of human peripheral blood mononuclear cells upon graphene stimulation. Others reported the obvious cytotoxicity of graphene and GO was often due to the good dispersion of graphene materials in cell culture medium and the substantial cellular uptake of the nanomaterials.[18] As for the graphene used in this study, it had poor dispersion in the cell culture medium and obvious aggregation was formed on the outer membrane of the cells after 24 h of exposure (Figure 4). Very little graphene was found in cells based on TEM searching (Figure 5). The cellular uptake of graphene could be hindered by both aggregation and the lamellar shape of graphene. Therefore, the poor solubility of graphene may block its potential toxic effects from an exogenous invader for cells. Similar results in the study by Mullick Chowdhury et al. showed that A549 cells had no uptake of graphene nanoribbons.[32] Jaworski et al. also pointed out that graphene platelets did not enter into the cells.[33] Nevertheless, as seen from Figure 4 and panels B–D of Figure 5, plenty of GS deposited closely to or attached on the cell membrane (indicated by the yellow arrow), which could pose direct stimulations to the cells through the physical contact.

Graphene-Activated EGFR/MAPK Signaling Pathways. We all know that the activation of members of the EGFR family is a kind of transmembrane tyrosine kinase. They play critical roles in regulating cell proliferation, differentiation, and migration.[34,35] Considering the phenotype of graphene-enhanced cellular proliferation and the membrane contact with graphene aggregates, it could be speculated that EGFR could

DOI: 10.1021/acs.jafc.5b05923
J. Agric. Food Chem. 2016, 64, 5909–5918

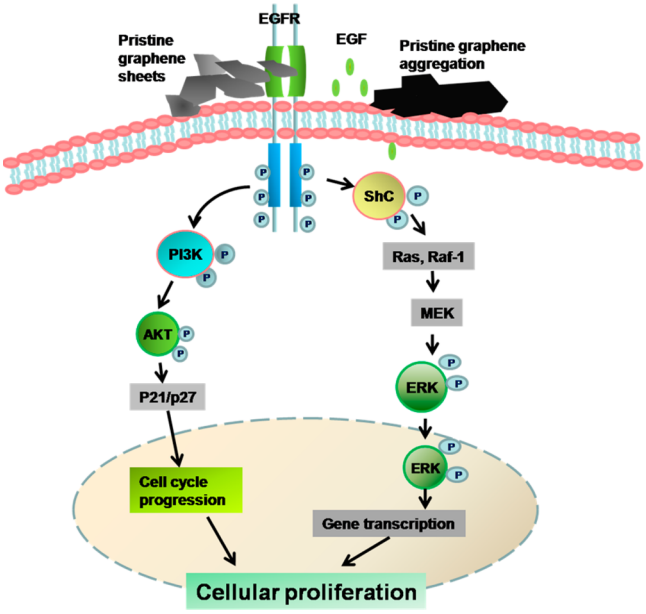

Figure 9. Schematic diagram delineating the mechanisms involved in graphene-enhanced cellular proliferation. The GS and aggregation triggered the EGFR by promoting EGF. Phosphorylated EGFR activated ShC and PI3 kinases, which upregulated downstream proteins ERK1/2 and AKT, modulated cell cycle progression and gene transcription, and eventually reinforced the cellular proliferation.

be influenced and involved in this biological process. Using HepG2 and A549 as the cell models, we evaluated the secretion of epidermal growth factor (EGF) in the cell culture medium after graphene stimulation using a commercially available enzyme-linked immunosorbent assay (ELISA) kit. A time-course study showed that extracellular EGF levels were significantly higher than the negative controls after 24 h of exposure of 40 μg/mL graphene ($p < 0.01$; Figure 6A). When the cells were treated with different concentrations of graphene (10−80 μg/mL), EGF secretion was significantly elevated with the increase of graphene stimulation doses in both cell lines (Figure 6B). This finding was well-consistent with the results from the cell proliferation indicated in Figure 2, suggesting that EGF could be the direct mediator for graphene-induced cell proliferation.

EGF, as one of the high-affinity ligands, can specially bind to EGFR, thus modulating cell survival and cell growth through the endogenous intricate signaling pathways.[36] The binding of EGF to the extracellular domain of EGFR induces the dimerization, activation of intrinsic kinase activity, and subsequent autophosphorylation of EGFR.[37] A western blot assay for graphene-treated HepG2 samples showed that the expression of phosphorylated EGFR was increased with the stimulation doses (Figure 7A). The induction of EGFR phosphorylation in graphene-treated cells was consistent with the finding of increased EGF secretion (Figure 6B).

Activated EGFR may recruit various cytoplasmic proteins and subsequently transduce the cellular impulse to exert function.[38] A series of protein recruitment phosphorylates MEKs, which then activates the ERK.[39] The graphene aggregated on the cell membrane could act as extracellular stimuli to upregulate the EGF, phosphorylate EGFR, and then activate the extracellular regulated kinases 1 and 2 (ERK1/2 or p44/42). Accordingly, ERK phosphorylation was also explored in this study, and the results were depicted in Figure 7A. Clearly, graphene treatment significantly elevated the levels of phosphorylated ERK, which was dose-dependent and well-matched with the result of EGFR phosphorylation.

Meanwhile, the phosphorylation of the modular protein ShC was found to be pronounced upregulated in graphene-treated cells and exhibited in a dose-related manner (Figure 7B). As reported, the association of ShC to EGFR may lead to its tyrosine phosphorylation and it is the main step in EGF-dependent induction of the MAPK pathway.[40] Thus, the phosphorylation of ShC in this result indicated the induction of the MAPK pathway upon treatment of graphene.

The activation of the ERK signaling pathway may modulate a number of transcriptional regulators to induce cell growth and proliferation.[41] In this study, we found PI3Ks, another major mediator in the EGFR signaling pathway, were also activated (Figure 7C). PI3Ks are major players in cellular functions, where they contribute to a variety of cellular processes, including proliferation, survival, adhesion, and migration.[42] Interaction between the PI3 kinase and the EGF receptors is required for its activation, and it is mediated by association of the phosphorylated receptors with the p85 subunit of PI3K.[43] PI3Ks convert phosphatidylinositol-4,5-bisphosphate (PIP2) to phosphatidylinositol-3,4,5-trisphosphate (PIP3). PIP3 binds to the PH domain of protein kinase B (PKB, also known as AKT) and recruits it to the plasma membrane. The phosphorylated AKT, in turn, regulates the activity of downstream proteins to mediate the cell survival.[44] It is a major mediator of PI3K action in survival and proliferation and may be the major mediator of the anti-apoptotic effects of EGFR activation.[45]

As shown in Figure 7C, the protein level of the p85 subunit of PI3K was elevated remarkably and the phosphorylation of AKT was prominent after the treatment of 10−40 μg/mL graphene, suggesting that the PI3K/AKT signal pathway be involved in the mechanism of graphene-induced proliferation. Studies showed that AKT appeared to regulate p27kip1 at multiple levels to ensure a tight control of progression through the G1 phase of the cell cycle.[46−48] As AKT was phosphorylated upon the treatment of graphene in our study, the G0/G1 arrest would be modulated by the activated AKT, which was confirmed by results from panels D and E of Figure 3.

We used miRNA-7 to block the expression of *EGFR*. miRNA-7 is a microRNA that inhibits *EGFR* by inducing mRNA decay.[49] Cells was transfected with miRNA-7 and negative control. The transfection efficiency was over 80% indicated by the negative control with Cy3 fluorescin, as shown in Figure S1 of the Supporting Information. After 24 h of transfection of miRNA-7, the expression of *EGFR* was significantly depressed (Figure 8A). In this case, graphene treatment did not stimulate expression of PI3K or Akt (Figure 8A). The proliferation of transfected cells was not enhanced by graphene treatment either (Figure 8B). To validate that EGFR involved in the mechanism of graphene induced cellular proliferation, we also investigated the cellular proliferation of the EGFR negative cell line CHO-K1 upon treatment of graphene. As shown in Figure 8C, no significant enhancement of cellular proliferation was observed in all groups treated with graphene. These results confirmed that the graphene induced cellular proliferation through activating EGFR.

This study investigated the toxicity of graphene on various cell lines. It found that the graphene enhanced the cellular proliferation and the transition of the cell cycle from the S phase to the G2/M phase. We also elucidated the molecular mechanisms responsible for graphene-enhanced cellular proliferation. As shown in the proposed schematic (Figure 9), we found

DOI: 10.1021/acs.jafc.5b05923
J. Agric. Food Chem. 2016, 64, 5909−5918

that the GS and aggregation attached on the cell membrane, promoted of EGF, and triggered the EGFR phosphorylation. The phosphorylated EGFR activated ShC and PI3 kinases, which upregulated downstream proteins ERK1/2 and AKT, modulated cell cycle progression and gene transcription, and eventually reinforced the cellular proliferation.

These results forecasted the cellular biological effects of graphene. It revealed the risk of graphene inducing cellular proliferation through MAPK/ERK and PI3K/AKT signal pathways. Further studies will focus on the verification of the graphene-induced cellular proliferation on *in vivo* models and investigate the possibility of cancerogenics induced by the activation of EGFR and AKT. We consider that the results from this study are significant for the application of graphene related with food.

■ ASSOCIATED CONTENT

Supporting Information

The Supporting Information is available free of charge on the ACS Publications website at DOI: 10.1021/acs.jafc.5b05923.

Expression of Cy3 fluorescin in HepG2 cells at 24 h after transfection (Figure S1) (PDF)

■ AUTHOR INFORMATION

Corresponding Authors

*E-mail: chenhm@aqsiqch.ac.cn.

*E-mail: zhouqf@rcees.ac.cn.

Funding

This research was supported by the Youth Foundation of Chinese Academy of Inspection and Quarantine (2013JK011 and 2016JK025), the Strategic Priority Research Program of the Chinese Academy of Science (14040302), the National Natural Science Foundation of China (21307124, 21522706, and 21107130), the Major International (Regional) Joint Project (21461142001), and the General Administration of Quality Supervision, Inspection and Quarantine (AQSIQ) of People's Republic of China (201510024).

Notes

The authors declare no competing financial interest.

■ REFERENCES

(1) Novoselov, K. S.; Geim, A. K.; Morozov, S. V.; Jiang, D.; Zhang, Y.; Dubonos, S. V.; Grigorieva, I. V.; Firsov, A. A. Electric field effect in atomically thin carbon films. *Science* **2004**, *306*, 666−669.

(2) Feng, L.; Liu, Z. Graphene in biomedicine: Opportunities and challenges. *Nanomedicine* **2011**, *6*, 317−324.

(3) Geim, A. K.; Novoselov, K. S. The rise of graphene. *Nat. Mater.* **2007**, *6*, 183−191.

(4) Arora, A.; Padua, G. W. Review: Nanocomposites in food packaging. *J. Food Sci.* **2010**, *75*, R43−R49.

(5) Kumar, S.; Ghosh, S.; Munichandraiah, N.; Vasan, H. 1.5 V battery driven reduced graphene oxide−silver nanostructure coated carbon foam (rGO−Ag−CF) for the purification of drinking water. *Nanotechnology* **2013**, *24*, 235101.

(6) Tu, Y.; Lv, M.; Xiu, P.; Huynh, T.; Zhang, M.; Castelli, M.; Liu, Z.; Huang, Q.; Fan, C.; Fang, H.; Zhou, R. Destructive extraction of phospholipids from Escherichia coli membranes by graphene nanosheets. *Nat. Nanotechnol.* **2013**, *8*, 594−601.

(7) Santos, C. M.; Mangadlao, J.; Ahmed, F.; Leon, A.; Advincula, R. C.; Rodrigues, D. F. Graphene nanocomposite for biomedical applications: Fabrication, antimicrobial and cytotoxic investigations. *Nanotechnology* **2012**, *23*, 395101.

(8) Akhavan, O.; Ghaderi, E. Toxicity of graphene and graphene oxide nanowalls against bacteria. *ACS Nano* **2010**, *4*, 5731−5736.

(9) Li, Y. T.; Qu, L. L.; Li, D. W.; Song, Q. X.; Fathi, F.; Long, Y. T. Rapid and sensitive in-situ detection of polar antibiotics in water using a disposable Ag-graphene sensor based on electrophoretic preconcentration and surface-enhanced Raman spectroscopy. *Biosens. Bioelectron.* **2013**, *43*, 94−100.

(10) Jian, J. M.; Liu, Y. Y.; Zhang, Y. L.; Guo, X. S.; Cai, Q. Fast and sensitive detection of Pb2+ in foods using disposable screen-printed electrode modified by reduced graphene oxide. *Sensors* **2013**, *13*, 13063−13075.

(11) Zhang, S.; Yang, K.; Feng, L.; Liu, Z. In vitro and in vivo behaviors of dextran functionalized graphene. *Carbon* **2011**, *49*, 4040−4049.

(12) Ruiz, O. N.; Fernando, K. A.; Wang, B.; Brown, N. A.; Luo, P. G.; McNamara, N. D.; Vangsness, M.; Sun, Y. P.; Bunker, C. E. Graphene oxide: A nonspecific enhancer of cellular growth. *ACS Nano* **2011**, *5*, 8100−8107.

(13) Depan, D.; Girase, B.; Shah, J. S.; Misra, R. D. Structure-process-property relationship of the polar graphene oxide-mediated cellular response and stimulated growth of osteoblasts on hybrid chitosan network structure nanocomposite scaffolds. *Acta Biomater.* **2011**, *7*, 3432−3445.

(14) Ryoo, S. R.; Kim, Y. K.; Kim, M. H.; Min, D. H. Behaviors of NIH-3T3 fibroblasts on graphene/carbon nanotubes: Proliferation, focal adhesion, and gene transfection studies. *ACS Nano* **2010**, *4*, 6587−6598.

(15) Chang, Y.; Yang, S. T.; Liu, J. H.; Dong, E.; Wang, Y.; Cao, A.; Liu, Y.; Wang, H. In vitro toxicity evaluation of graphene oxide on A549 cells. *Toxicol. Lett.* **2011**, *200*, 201−210.

(16) Wang, K.; Ruan, J.; Song, H.; Zhang, J.; Wo, Y.; Guo, S.; Cui, D. Biocompatibility of graphene oxide. *Nanoscale Res. Lett.* **2010**, *6*, 1−8.

(17) Zhang, Y.; Ali, S. F.; Dervishi, E.; Xu, Y.; Li, Z.; Casciano, D.; Biris, A. S. Cytotoxicity effects of graphene and single-wall carbon nanotubes in neural phaeochromocytoma-derived PC12 cells. *ACS Nano* **2010**, *4*, 3181−3186.

(18) Qu, G.; Liu, S.; Zhang, S.; Wang, L.; Wang, X.; Sun, B.; Yin, N.; Gao, X.; Xia, T.; Chen, J.-J.; Jiang, G.-B. Graphene oxide induces toll-like receptor 4 (TLR4)-dependent necrosis in macrophages. *ACS Nano* **2013**, *7*, 5732−5745.

(19) Seabra, A. B.; Paula, A. J.; de Lima, R.; Alves, O. L.; Duran, N. Nanotoxicity of graphene and graphene oxide. *Chem. Res. Toxicol.* **2014**, *27*, 159−168.

(20) Eriksen, J. L.; Druse, M. J. Astrocyte-mediated trophic support of developing serotonin neurons: Effects of ethanol, buspirone, and S100B. *Dev. Brain Res.* **2001**, *131*, 9−15.

(21) Mosmann, T. Rapid colorimetric assay for cellular growth and survival: Application to proliferation and cytotoxicity assays. *J. Immunol. Methods* **1983**, *65*, 55−63.

(22) Liu, S.; Goldstein, R. H.; Scepansky, E. M.; Rosenblatt, M. Inhibition of Rho-Associated Kinase Signaling Prevents Breast Cancer Metastasis to Human Bone. *Cancer Res.* **2009**, *69*, 8742−8751.

(23) Graf, D.; Molitor, F.; Ensslin, K.; Stampfer, C.; Jungen, A.; Hierold, C.; Wirtz, L. Spatially resolved Raman spectroscopy of single- and few-layer graphene. *Nano Lett.* **2007**, *7*, 238−242.

(24) Ferrari, A. C.; Basko, D. M. Raman spectroscopy as a versatile tool for studying the properties of graphene. *Nat. Nanotechnol.* **2013**, *8*, 235−246.

(25) Sanchez, V. C.; Jachak, A.; Hurt, R. H.; Kane, A. B. Biological interactions of graphene-family nanomaterials—An interdisciplinary review. *Chem. Res. Toxicol.* **2012**, *25*, 15−34.

(26) Nurunnabi, M.; Khatun, Z.; Huh, K. M.; Park, S. Y.; Lee, D. Y.; Cho, K. J.; Lee, Y.-k In Vivo Biodistribution and Toxicology of Carboxylated Graphene Quantum Dots. *ACS Nano* **2013**, *7*, 6858−6867.

(27) Yang, K.; Wan, J.; Zhang, S.; Zhang, Y.; Lee, S.-T.; Liu, Z. In Vivo Pharmacokinetics, Long-Term Biodistribution, and Toxicology of PEGylated Graphene in Mice. *ACS Nano* **2011**, *5*, 516−522.

(28) Zhang, X.; Yin, J.; Peng, C.; Hu, W.; Zhu, Z.; Li, W.; Fan, C.; Huang, Q. Distribution and biocompatibility studies of graphene oxide in mice after intravenous administration. *Carbon* **2011**, *49*, 986−995.

(29) Yang, K.; Zhang, S.; Zhang, G.; Sun, X.; Lee, S.-T.; Liu, Z. Graphene in Mice: Ultrahigh In Vivo Tumor Uptake and Efficient Photothermal Therapy. *Nano Lett.* **2010**, *10*, 3318−3323.
(30) Liao, K. H.; Lin, Y. S.; Macosko, C. W.; Haynes, C. L. Cytotoxicity of graphene oxide and graphene in human erythrocytes and skin fibroblasts. *ACS Appl. Mater. Interfaces* **2011**, *3*, 2607−2615.
(31) Sasidharan, A.; Panchakarla, L. S.; Sadanandan, A. R.; Ashokan, A.; Chandran, P.; Girish, C. M.; Menon, D.; Nair, S. V.; Rao, C. N.; Koyakutty, M. Hemocompatibility and macrophage response of pristine and functionalized graphene. *Small* **2012**, *8*, 1251−1263.
(32) Mullick Chowdhury, S.; Manepalli, P.; Sitharaman, B. Graphene nanoribbons elicit cell specific uptake and delivery via activation of epidermal growth factor receptor enhanced by human papillomavirus E5 protein. *Acta Biomater.* **2014**, *10*, 4494−4504.
(33) Jaworski, S.; Sawosz, E.; Grodzik, M.; Winnicka, A.; Prasek, M.; Wierzbicki, M.; Chwalibog, A. In vitro evaluation of the effects of graphene platelets on glioblastoma multiforme cells. *Int. J. Nanomed.* **2013**, *8*, 413−420.
(34) Ushiro, H.; Cohen, S. Identification of phosphotyrosine as a product of epidermal growth factor-activated protein kinase in A-431 cell membranes. *J. Biol. Chem.* **1980**, *255*, 8363−8365.
(35) Schreiber, A. B.; Libermann, T. A.; Lax, I.; Yarden, Y.; Schlessinger, J. Biological role of epidermal growth factor-receptor clustering. Investigation with monoclonal anti-receptor antibodies. *J. Biol. Chem.* **1983**, *258*, 846−853.
(36) Teramura, Y.; Ichinose, J.; Takagi, H.; Nishida, K.; Yanagida, T.; Sako, Y. Single-molecule analysis of epidermal growth factor binding on the surface of living cells. *EMBO J.* **2006**, *25*, 4215−4222.
(37) Moriki, T.; Maruyama, H.; Maruyama, I. N. Activation of preformed EGF receptor dimers by ligand-induced rotation of the transmembrane domain. *J. Mol. Biol.* **2001**, *311*, 1011−1026.
(38) Real, F. X.; Rettig, W. J.; Chesa, P. G.; Melamed, M. R.; Old, L. J.; Mendelsohn, J. Expression of epidermal growth factor receptor in human cultured cells and tissues: Relationship to cell lineage and stage of differentiation. *Cancer Res.* **1986**, *46*, 4726−4731.
(39) Iwamoto, E.; Ueta, N.; Matsui, Y.; Kamijo, K.; Kuga, T.; Saito, Y.; Yamaguchi, N.; Nakayama, Y. ERK plays a role in chromosome alignment and participates in M-phase progression. *J. Cell. Biochem.* **2016**, *117*, 1340−1351.
(40) Sakaguchi, K.; Okabayashi, Y.; Kido, Y.; Kimura, S.; Matsumura, Y.; Inushima, K.; Kasuga, M. Shc phosphotyrosine-binding domain dominantly interacts with epidermal growth factor receptors and mediates Ras activation in intact cells. *Mol. Endocrinol.* **1998**, *12*, 536−543.
(41) Pages, G.; Lenormand, P.; L'Allemain, G.; Chambard, J. C.; Meloche, S.; Pouyssegur, J. Mitogen-activated protein kinases p42mapk and p44mapk are required for fibroblast proliferation. *Proc. Natl. Acad. Sci. U. S. A.* **1993**, *90*, 8319−8323.
(42) Kriplani, N.; Hermida, M. A.; Brown, E. R.; Leslie, N. R. Class I PI 3-kinases: Function and evolution. *Adv. Biol. Regul.* **2015**, *59*, 53−64.
(43) Jorissen, R. N.; Walker, F.; Pouliot, N.; Garrett, T. P.; Ward, C. W.; Burgess, A. W. Epidermal growth factor receptor: Mechanisms of activation and signalling. *Exp. Cell Res.* **2003**, *284*, 31−53.
(44) Kandasamy, K.; Mohan, S. S.; Raju, R.; Keerthikumar, S.; Kumar, G. S.; Venugopal, A. K.; Telikicherla, D.; Navarro, J. D.; Mathivanan, S.; Pecquet, C.; Gollapudi, S. K.; Tattikota, S. G.; Mohan, S.; Padhukasahasram, H.; Subbannayya, Y.; Goel, R.; Jacob, H. K.; Zhong, J.; Sekhar, R.; Nanjappa, V.; Balakrishnan, L.; Subbaiah, R.; Ramachandra, Y. L.; Rahiman, B. A.; Keshava Prasad, T. S.; Lin, J. X.; Houtman, J. C.; Desiderio, S.; Renauld, J. C.; Constantinescu, S. N.; Ohara, O.; Hirano, T.; Kubo, M.; Singh, S.; Khatri, P.; Draghici, S.; Bader, G. D.; Sander, C.; Leonard, W. J.; Pandey, A. NetPath: A public resource of curated signal transduction pathways. *Genome Biol.* **2010**, *11*, R3.
(45) Mattoon, D. R.; Lamothe, B.; Lax, I.; Schlessinger, J. The docking protein Gab1 is the primary mediator of EGF-stimulated activation of the PI-3K/Akt cell survival pathway. *BMC Biol.* **2004**, *2*, 24.
(46) Burgering, B. M. T.; Medema, R. H. Decisions on life and death: FOXO Forkhead transcription factors are in command when PKB/Akt is off duty. *J. Leukocyte Biol.* **2003**, *73*, 689−701.
(47) Sanchez, I.; Dynlacht, B. D. New insights into cyclins, CDKs, and cell cycle control. *Semin. Cell Dev. Biol.* **2005**, *16*, 311−321.
(48) Sun, B.; Geng, S.; Huang, X.; Zhu, J.; Liu, S.; Zhang, Y.; Ye, J.; Li, Y.; Wang, J. Coleusin factor exerts cytotoxic activity by inducing G0/G1 cell cycle arrest and apoptosis in human gastric cancer BGC-823 cells. *Cancer Lett.* **2011**, *301*, 95−105.
(49) Webster, R. J.; Giles, K. M.; Price, K. J.; Zhang, P. M.; Mattick, J. S.; Leedman, P. J. Regulation of epidermal growth factor receptor signaling in human cancer cells by microRNA-7. *J. Biol. Chem.* **2009**, *284*, 5731−5741.

DOI: 10.1021/acs.jafc.5b05923
J. Agric. Food Chem. 2016, 64, 5909−5918